

Experimental investigation on the tensile behavior of grouted sleeve connections under different thermal and mechanical loads

Tan Wang^a, Haoming Xu^a, Min Yu^{a,c,*}, Lihua Xu^a, Jianqiao Ye^{b,*}

a. School of Civil Engineering, Wuhan University, Wuhan 430072, China;

b. Department of Engineering, Lancaster University, Lancaster, LA1 4YR. UK;

c. Engineering Research Center of Urban Disasters Prevention and Fire Rescue Technology of Hubei Province, Wuhan 430072, China;

Abstract: Grouted sleeve connections are widely used in precast concrete structures for joining rebar. In order to understand the behavior of grouted sleeves under and after fire, tensile tests were carried out on grouted sleeves with threaded bars under three different thermo-mechanical loading conditions, including applying load when temperature is constant, heating when a constant mechanical load is maintained and applying mechanical loads at room temperature on previously heated grooves. Tensile tests of continuous rebar were also conducted for comparisons. Failure modes and degradation of mechanical properties of both grouted sleeve connections and continuous rebar subjected to above conditions were studied. It was found that temperature resistances of grouted sleeve connections with or without considering heating process were significantly different, while such differences were negligible for continuous rebar. It was also found that grouted sleeve connections could restore some of the mechanical capacities after they were cooled down to room temperature. Finally, predictive models were proposed for potential adoption in fire resistance design and post fire evaluation of grouted sleeve connections.

Keywords: Grouted sleeves connection; Temperature-load paths; Failure mode; Tensile behavior; Calculation method

Notations

$\bar{f}_{y,G}, \bar{f}_{yT,G}, \bar{f}_{yTp,G}$	equivalent yield strength of grouted sleeve connection at ambient temperature, elevated temperature and after elevated temperature, respectively
$\bar{f}_{u,G}, \bar{f}_{uT,G}, \bar{f}_{uTp,G}$	equivalent ultimate strength of grouted sleeve connection at ambient temperature, elevated temperature and after elevated temperature, respectively
$\bar{E}_{s,G}, \bar{E}_{sT,G}, \bar{E}_{sTp,G}$	equivalent elastic modulus of grouted sleeve connection at ambient temperature, elevated temperature and after elevated temperature, respectively
$f_{y,r}, f_{yT,r}, f_{yTp,r}$	yield strength of rebar at ambient temperature, elevated temperature and after elevated temperature, respectively
$f_{u,r}, f_{uT,r}, f_{uTp,r}$	ultimate strength of rebar at ambient temperature, elevated temperature and after elevated temperature, respectively

$E_{s,r}, E_{sT,r}, E_{sTp,r}$	elastic modulus of rebar at ambient temperature, elevated temperature and after elevated temperature, respectively
$f_{cu,g}, f_{cuT,g}, f_{cuTp,g}$	ultimate strength of grouting material at ambient temperature, elevated temperature and after elevated temperature, respectively
$\varepsilon_r, \varepsilon_G, \varepsilon_g$	relative expansion strain of rebar, grouted splice sleeve connection and grouting material, respectively
A_r, A_g, A_s	area of rebar, grout and sleeve, respectively
l_0, l_T	length of ambient and elevated temperature section, respectively
$\bar{\varepsilon}$	equivalent strain $\bar{\varepsilon} = \Delta l_T / l_T$
σ	axial stress applied on specimen
n	load ratio $n = \sigma / f_{s,y}$
r	heating rate
T	temperature
T_c	critical temperature
t	heating time
d	diameter of rebar

1. Introduction

Grouted sleeves connections with advantages of simple operation and reliable joint performance are widely used in precast concrete structures for joining rebars. The mechanical performance of some precast concrete structures with grouted sleeve connections were studied in the past decade, including beam-column connections^[1], shear walls^[2], columns-to-column connections^[3] and column-to-foundation connections^[4]. It was found that the mechanical behavior of the integrated structures was clearly affected by the grouted sleeve connections. In this respect, some researchers have conducted thorough and systematic studies on the mechanical behavior of grout sleeve connections. The parameters investigated include the shape of sleeves^[5,6], rebar offset^[7], bar size^[8], head attached to the bar^[9] and grouting materials^[10]. These studies have shown that the strength of a grouted sleeve connecting two rebars can be higher than that of the individual rebar if the sleeve connection is properly designed. Design standards and guidelines^[11-13] are now available to provide design requirement for grout sleeve connections.

It is evident that recent research on the behavior of grout sleeve connections subject to normal ambient temperature has made significant progress and achieved fruitful results. However, modern practices often require reasonably robust design for structures under fire and for strengthening structures damaged by fire. This demands further research as the properties of rebar^[14-21], cement-based materials^[22-24] and their interactions^[25-27] at elevated temperature are all significantly different, resulting in different mechanical behavior of grouted sleeve connections. Zhao^[28], Wang^[29], Zhang^[30] studied tensile behavior of a half grouted sleeve connection subjected to uniform temperature and found that the failure mode of the half grouted sleeve connection was temperature dependent.

This dependence may become more complicated as, in a real fire situation, the temperature distribution in the structure is not uniform, leading to different thermal expansion and thermo-mechanical responses of the material at different positions. It will not be sufficiently reliable to investigate fire behavior of grouted sleeve connections by considering uniform temperature. Furthermore, assessment of fire damage, such as residual strength of a connection, is also a critical issue. Currently, research on the mechanical behavior of grouted sleeve connections under various combination of thermal and mechanical loadings are rarely available.

In order to systematically understand the tensile behavior of grouted sleeves under different thermo-mechanical conditions, the following three different load-temperature paths were considered in this research, including, Path-I: applying load when temperature is constant; Path-II: heating when a constant load is maintained; and Path-III: applying load after the connections were heated and cooled down to room temperature. For comparisons, tensile tests of continuous rebars were also conducted under the three load-temperature paths, respectively. The failure modes, mechanical properties of the grouted sleeve connections and the comparison with continuous rebars were studied. Finally, models for predicting mechanical properties of grouted sleeve connections were proposed.

2. Experimental program

2.1 Experimental design and specimens

2.1.1 Experimental design

In this paper, the test results of 33 grouted sleeve connections and 33 continuous rebars are reported for the three load-temperature paths mentioned in Section one, namely, Path-I: applying load when temperature is constant, which is to study the high temperature behavior of the specimens under constant temperature; Path-II: heating when a constant load is maintained, which is to simulate the behavior of specimens in real fire condition; and Path-III: applying load after the connections were heated and cooled down to room temperature, which is used to study the effect of temperature history on the behavior of the specimens. Graphic illustrations of the three paths are shown in Figure 1.

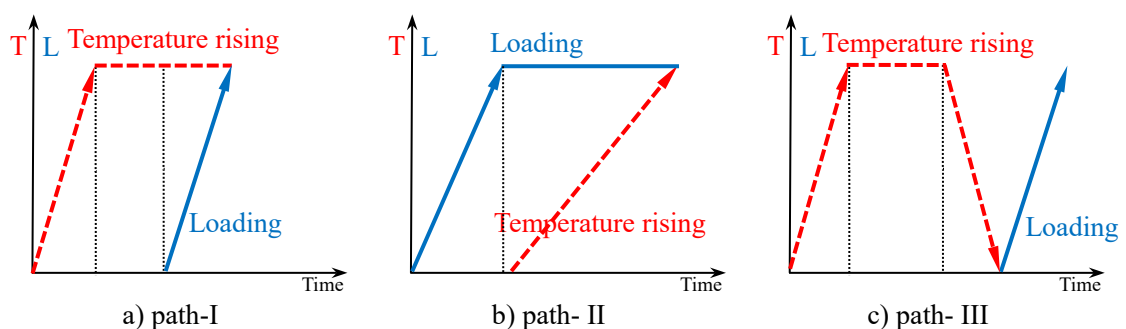


Figure 1 Sketch of the different temperature-load paths

Nine grouted sleeve connections and 9 continuous rebars were tested subjected to Path-I loading at, respectively, 9 different constant temperature, i.e., 20°C, 100°C, 200°C, 300°C, 400°C, 500°C, 600°C, 700°C, and 800°C. 15 grouted sleeve connections and 15 continuous rebars were tested for Path-II with a load ratio, $n = \sigma / f_{s,y}$, where σ is the axial stress applied on a

specimen and $f_{s,y}$ is the equivalent yield strength of the specimen, of 0.5, 0.6, 0.7, 0.8, 0.9, respectively. The equivalent heating rate (to be defined later) is 7.5°C/min, 14.3°C/min and 21.1°C/min. For Path-III, 9 grouted sleeve connections and 9 continuous rebars were tested. The connections were heated up to, respectively, 20°C, 100°C, 200°C, 300°C, 400°C, 500°C, 600°C, 700°C, and 800 °C. All the grouted sleeve connections are circular, having a diameter of 46 mm and a sleeve of 2.5mm thick. The length of the connection is 275mm and the rebar outside the sleeve is 190mm long at both ends, as shown in Figure 2.

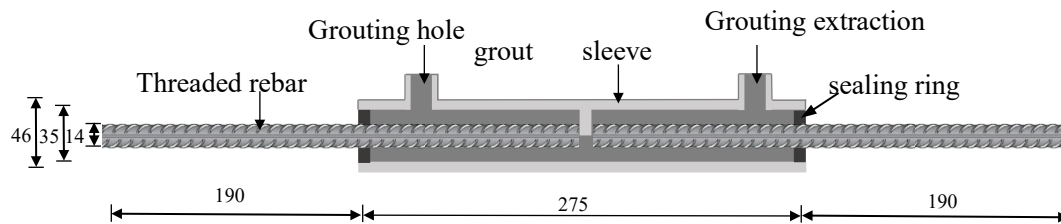


Figure 2 Dimension of test specimen

The GT14L fully-grouted sleeve with a tensile strength of 600MPa, which meets the requirements of technical specifications of JGJ107^[11] and JG/T 398^[12], was chosen in this study to connect tapered rebars of diameter 14mm and made of steel grade HRB400. The measured strength of the threaded rebar at room temperature was 428MPa. The threaded rebar was cut to 320mm long according to the Chinese Standards^[11] and the dimensions of the furnace. The CGMJM-VIII cementitious grout, which meets the requirements of Chinese Specifications JG/T408^[13], was used. The measured strength of the grout after 28 days at room temperature was 114.95 MPa.

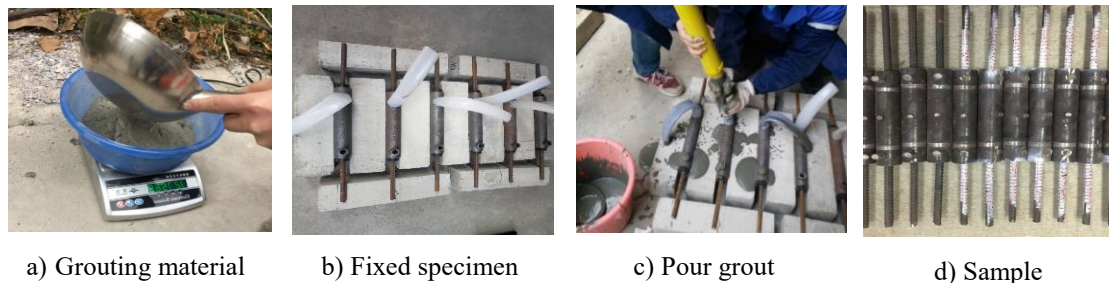


Figure 3 Fabrication process of specimens

Prior to grouting, two threaded rebars were inserted into the ends of a sleeve and effort was made to ensure that the axes of the rebars were align to the axis of the sleeve. Cementitious grout with water cement ratio of 13:1 was injected into the sleeve by a grout pump through the grouting hole until excessive grout was pushed out from the grouting extraction hole. Two sealing rings were mounted at both ends of the sleeve to prevent grout leaking. The fabrication process of specimens can be seen in Figure 3.

2.2 Test set-up and methodology

2.2.1 Test set-up

The fire tests were carried out at the Laboratory of Materials and Structures under Extreme Environment, Wuhan University in China. A universal test machine, a GW900 electrical furnace and an Imetrum non-contact Digital Image Correlation (DIC) measuring system were used to

record the performance of the connections when they were subjected both thermal and mechanical loadings. Figure 4 shows the set-up of a test where Figure 4(a) is a photo showing the overall arrangement of the test and Figure 4(b) is a sectional view of the furnace.

The servo universal test machine has a maximum loading capacity of 300 KN with a precision of $\pm 0.5\%$. The GW900 furnace is capable of simulating temperatures up to 1200 °C ($\pm 3^{\circ}\text{C}$). The temperature inside the furnace was measured by taking average of three thermocouples located at three different positions.

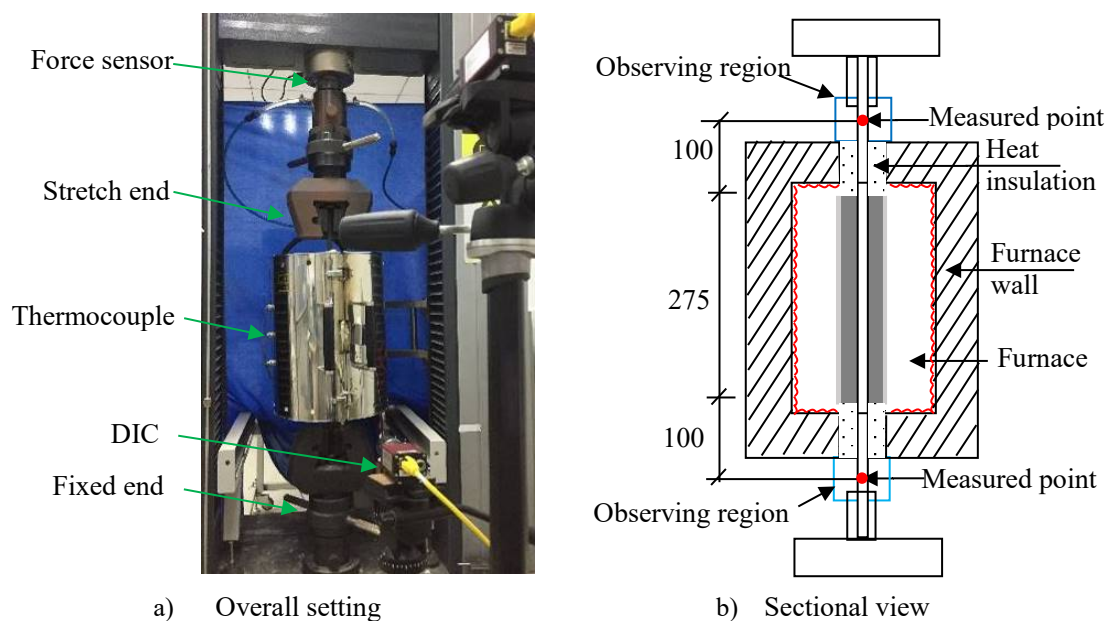


Figure 4 Test set-up and instruments

Compared to the traditional displacement measurement through direct contact, the no-contact displacement measurement system is advantageous in high temperature tests. The DIC systems provides accurate and continuous multiple point-to-point measurements of displacements of a region.

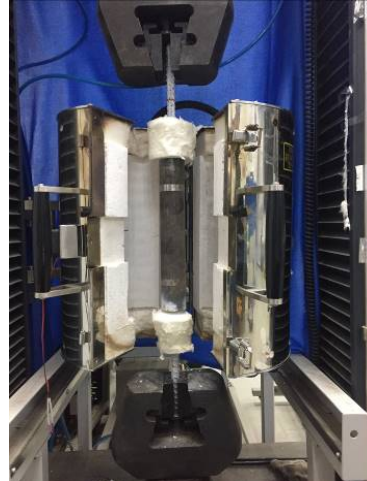
2.2.2 Test methodology

As shown in Figure 1, under Path-I, the specimens were heated to a specific temperature at a heating rate of $10^{\circ}\text{C}/\text{min}$. The temperature was maintained for 3 hours so that a uniform temperature field was achieved in the furnace. The specimens were then stretched at a speed of $1.2\text{mm}/\text{min}$ until they failed. During the heating stage, the specimens were not fully restrained to allow free expansion. Under Path-II, the specimens were stretched at a speed of $100\text{N}/\text{s}$ to a specific load level and were then heated at a heating rate until the specimen failed. Under Path-III, the specimens were heated to a targeting temperature at a heating rate of $10^{\circ}\text{C}/\text{min}$. The temperature was maintained for 3 hours. The specimens were cooled down to the room temperature and stretched then at $1.2\text{mm}/\text{min}$ until the specimen failed.

The deformation and tensile force were measured from all the tests. The critical temperature, at which a specimen breaks, was also measured under Path-II. In the fire tests, it was difficult to measure the deformation of the specimen inside the furnace directly. Based on the deformation modification method^[31], the deformation of a specimen inside the furnace was obtained by modifying the deformation between two measured points out of the furnace.



a) Connection and rebar



c) Connection

Figure 5 Heated area of specimens

It was observed that if the heated area includes both connection and parts of outside rebar, as shown in Figure 5(a), all the specimens finally failed due to the failure of the rebar. Thus, in order to study failure of a connection, the rebar inside the furnace was insulated from high temperature so that only the connection was heated during the test, as shown in Figure 5(b).

3. Experimental results and discussion

3.1 Loading under constant temperature (Path-I)

3.1.1 Failure mode

Possible failure modes under Path-I load include bond failure (Figure 6a) and rebar rapture. Rebar rapture occurred both outside (Fig.6b) and inside (Fig.6c) the sleeve.



a) Bond-slip failure



b) Outside rebar rapture



c) Inside rebar rapture near the sleeve end

Figure 6 Final failure mode under Path- I

When the temperature outside the sleeve is below 400°C, the sleeve fails due to outside rebar rapture (Fig.6b) when the applied tensile strength exceeds the strength of the steel rebar at room temperature. The bond strength between the rebar and the grout is gradually reduced as the temperature continued to increase. However, at this stage, the overall strength of the sleeve connection is still stronger than the strength of steel rebar at room temperature. When the outside

temperature reaches 500 °C, bond failure (Fig.6a) occurs once the bond stress exceeds the bond strength. The bond strength between the rebar and the grout decreases rapidly and gradually so that the overall strength of the sleeve connection become weaker than the strength of rebar at room temperature.

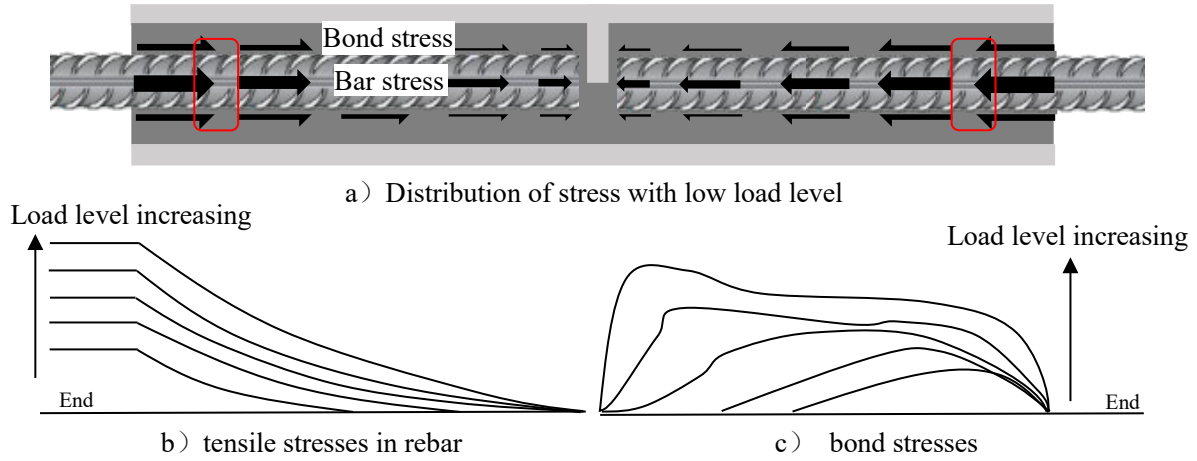


Figure 7 Stress inside the connection

When the outside temperature exceeds 500°C, all specimens fail due to rebar rapture occurs inside and near the top end of the sleeves. Figure 7 illustrates the distribution of tensile stresses in the rebar and shear stresses along the bond inside the sleeve [31]. It is found that the maximum tensile stress of rebar inside the sleeve occurred near the sleeve edge and is slightly smaller than the stress of the rebar away from the connection. However, the rebar inside the connection is always subjected to a higher temperature in the test, and prone to fail earlier. Therefore, all failure occurred near the top end of the sleeves.

3.1.2 Comparison with continuous rebar

In this Section, the equivalent strain-stress relations, tensile strengths and elastic modulus of the grouted sleeve connections under elevated temperature are compared with those of continuous rebar, as shown in Figures 8 and 9. The test results shown in the figures were obtained under load Path-I.

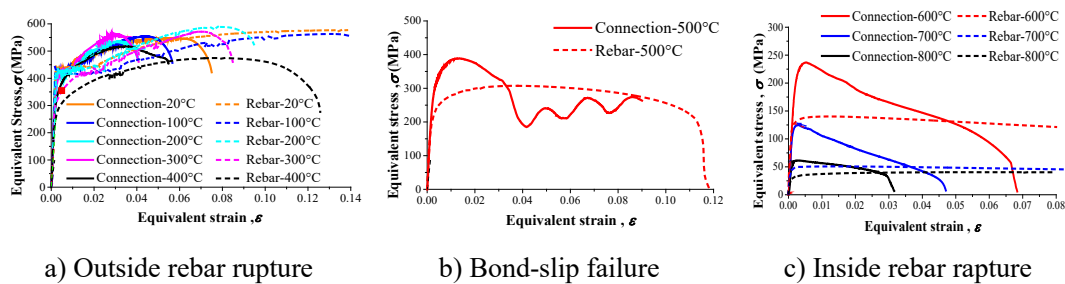


Figure 8 Stress-strain curves under path-I

For a connection or a continuous rebar fails due to rebar rapture, if there is an obvious yield plateau in the stress-strain curve, the equivalent yield strength is defined as the lower yield point. Otherwise, the 0.2% offset yield strength applies. For a connection with bond failure model, the equivalent yield strength is the stress that causes first sudden increase of strain. For all the cases, the equivalent ultimate stress is the maximum stress of a stress-strain curve, and the equivalent

elastic modulus is calculated from the initial slope of the stress-strain curves.

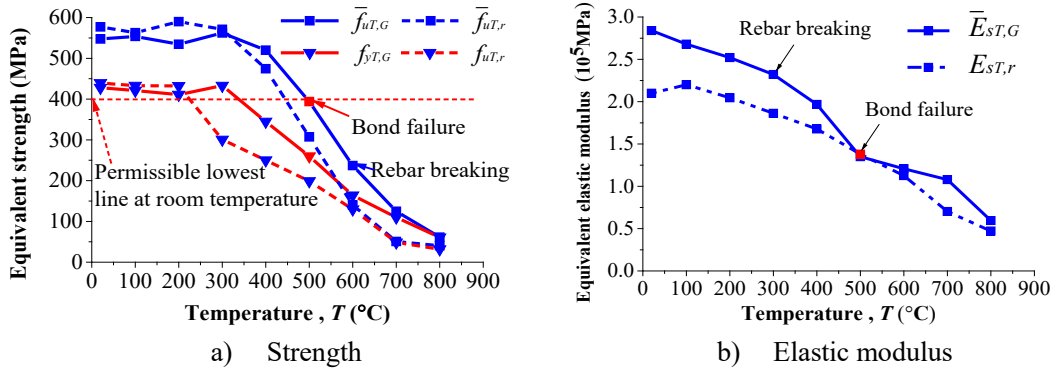


Figure 9 Comparison of mechanical properties between grouted sleeve and continuous rebar under Path-I

In the above Figures, $\bar{f}_{yT,G}$ and $\bar{f}_{uT,G}$ are equivalent yield strength and ultimate strength of a grouted sleeve connection at elevated temperature, respectively; $\bar{f}_{yT,r}$ and $\bar{f}_{uT,r}$ are yield strength and ultimate strength of a continuous rebar at elevated temperature, respectively; $\bar{E}_{sT,G}$ and $E_{sT,r}$ are equivalent elastic modulus of a grouted sleeve connection and elastic modulus of a continuous rebar at elevated temperature, respectively.

As shown in Figure 9 (a), when the heating temperature is below 400 °C, the connections fail due to rebar rupture outside the connections, thus, the strength of the grouted sleeve connections is the same as that of a continuous rebar at room temperature. The ultimate strength of the sleeves is also the same as that of the continuous rebar under room temperature. When the heating temperature exceeds 400 °C, the equivalent ultimate strength of the grouted sleeve connections is always greater than that of the continuous rebar. It can be concluded that under load Path-I the sleeve connection is unlikely to fail first, independent of temperature. Thus, it is recommended that for Path-I design the strength of continuous rebar should be used as the strength of a grouted sleeve connection at elevated temperature. As shown also in Figure 9 (b), the elastic modulus of the grouted sleeve connections is always greater than that of continuous rebar since the slip between rebar and grout was very small in the elastic stage.

3.2 Heating under constant load (Path-II)

3.2.1 Failure mode

Figure 10 shows failure mode of a sleeve connection under load Path-II. Because both the tensile strength of rebar and the bond strength are reduced due to rebar softening and bond degradation when the heating temperature exceeds 500°C, the inside rebar ruptured near the edge of the sleeve. The detailed analyses of the failure can be seen in Section 3.1.

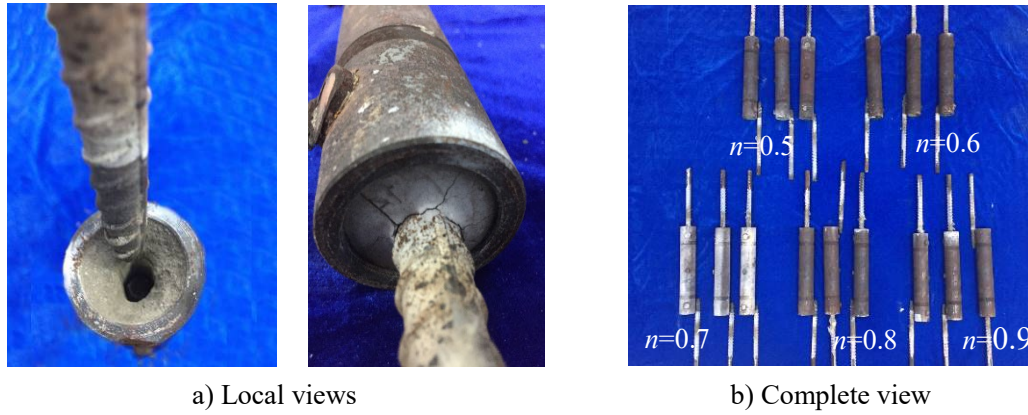


Figure 10 Failure mode under path-II

3.2.2 The influence of load level and heating rate

In a real fire situation, the rebar at different positions in a structure are subjected to different loads and heating rates. In this Section, load ratio, n , and heating rate r are studied to understand fire resistance of the connection under Path-II. The load ratio n ranges from 0.5 to 0.9 at every 0.1. As shown in Figure 11, the equivalent heating rate calculated from the equal area method^[32], which equates the area under the actual heating rate curve to the one under the equivalent heating rate curve, are $7.5^{\circ}C/min$, $14.3^{\circ}C/min$ and $21.1^{\circ}C/min$, respectively. To save the space and without loss of generality, Figures 12 (a) and (b) show only the influence of heating rate under load ratio $n = 0.5$ and the influence of load ratio under heating rate $r = 14.3^{\circ}C/min$, respectively, on the temperature-equivalent strain relations.

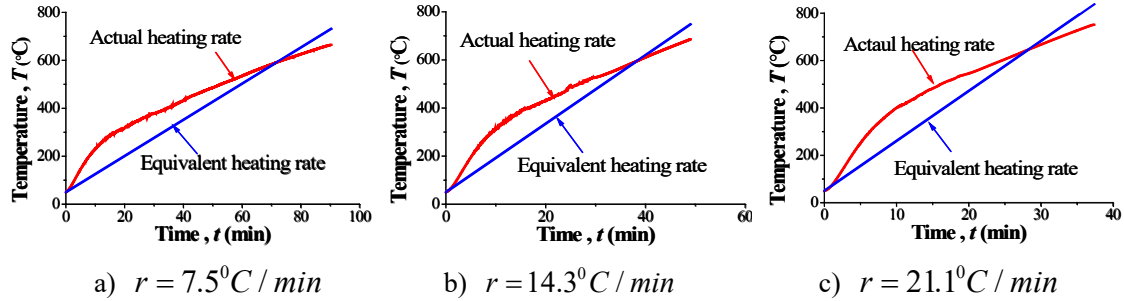


Figure 11 Time-temperature curve in the furnace

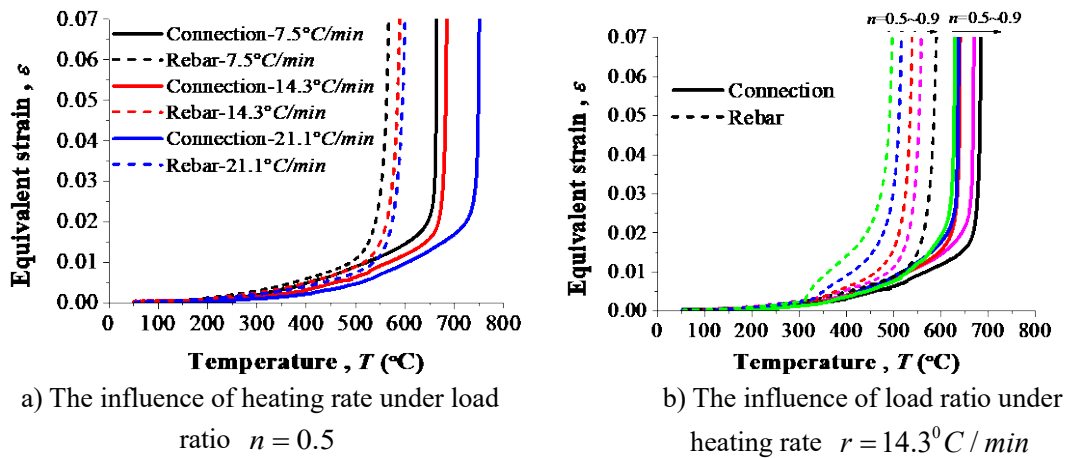


Figure 12 Temperature via equivalent strain of grouted sleeve connections and continuous rebar under Path-II

It can be seen from Figure (12) that the strain of the connection increases exponentially as the temperature increases. The equivalent strain of the connection, which consists of bond-slip and elongation of rebar, is less than the strain of a continuous rebar due to the fact that under the same load the stress in the continuous rebar is far greater than that of the rebar inside the connection.

For the grouted sleeve connections with the same load ratio, a lower heating rate results in greater strain at the same temperature. This is because more time is required to reach the targeting temperature when the heating rate is lower, thus more creep strain will occur. Under the same heating rate and temperature, the grouted sleeve connections have greater strain when the load ratio is higher. This is not obvious in the early stage of heating until the temperature is higher when the creep strain of sleeve become significant. All above observations apply also to the strain of continuous rebar.

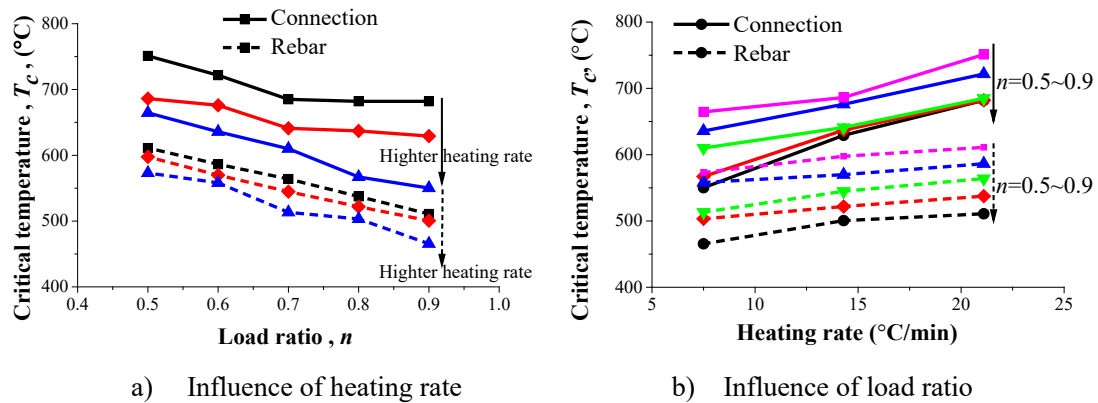


Figure 13 Influence of heating rate and load ratio on critical temperature

Figure 13 shows the influence of heating rate and load ratio on the critical temperature, T_c , of the connections and continuous rebar. When they are under the same heating rate, the higher the load level is, the lower the critical temperature will be. When they are subjected to the same load ratio, a higher heating rate always results in a higher critical temperature. It can be found that a grouted sleeve connection has enhanced temperature performance than a continuous rebar does, which is attributed mainly to: (a) the stress of the rebar inside the grouted sleeve connection is smaller than that of a continuous rebar due to the bond that redistributes the stress, and (b) compared to rebar outside the sleeve, more time is required for the core of the grouted sleeve connection to reach the same temperature due to the reduced thermal conductivity. It can also be found that the effect of heating rate on the high temperature performance of the grouted sleeve connections was more obvious than that of continuous rebar, as the rate affects the temperature gradient across the section of the grouted sleeves.

3.3 Loading after elevated temperature (Path- III)

3.3.1 Failure mode

The primary failure modes of a grouted sleeve connection under load path-III are rebar rupture outside the connection and bond failure, which are shown in Figure 14.



a) Rebar rapture outside the connection

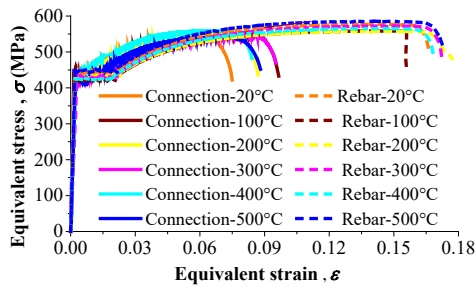
a) Bond failure

Figure 14 Failure modes under path-III

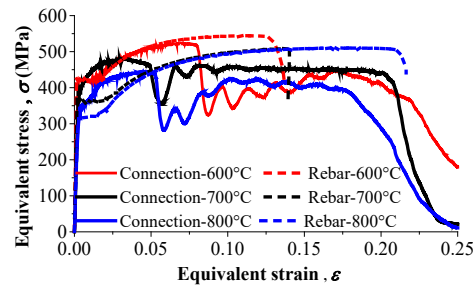
For a grouted sleeve cooled down from a peak temperature below 500°C, failure occurs due to rebar rapture outside the connection (Fig.14a) as the stress in the rebar exceeds the tensile strength first, which is an ideal failure mode (no connection failure) in practical application. When the peak temperature exceeds 500 °C, the sleeve fails due to bond failure as the bond stress exceeds bond strength between the rebar and the grouting material. When the peak temperature ranges from 600°C to 800°C, the effect of temperature history on the bond strength is obvious. The overall strength of sleeve connection is weaker than the tensile strength of the rebar under higher experienced temperature.

3.3.2 Comparisons with continuous rebar

Comparisons of equivalent strain-stress, strength and elastic modules between the grouted sleeves and continuous rebar under Path-III are shown in Figure 15 and Figure 16, respectively.

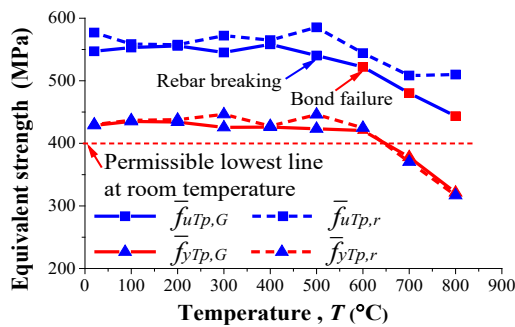


a) Rebar rapture outside the connection

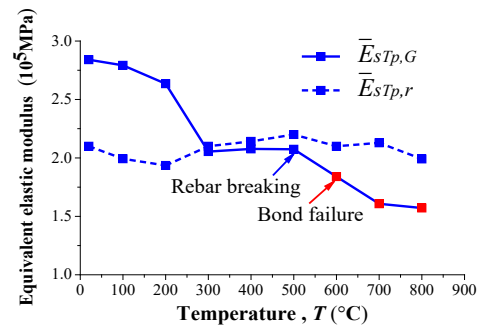


b) Bond failure

Figure 15 Equivalent strain-stress curve under path-III



a) Strength



b) Elastic, modulus

Figure 16 Comparison of mechanical properties between grouted sleeves connection and

continuous rebar under Path-III

In the above figures, $\bar{f}_{yTp,G}$ and $\bar{f}_{uTp,G}$ are equivalent yield strength and equivalent ultimate strength of a grouted sleeve connection after elevated temperature, respectively; $\bar{f}_{yTp,r}$, $\bar{f}_{uTp,r}$ are equivalent yield strength and equivalent ultimate strength of a continuous rebar after elevated temperature, respectively; $\bar{E}_{sTp,G}$, $E_{sTp,r}$ are equivalent elastic modulus of a grouted sleeve connection and elastic modulus of a continuous rebar after elevated temperature, respectively.

When the peak temperature from which the specimens were cooled down was below 500 °C, the connections fail due to rebar rupture outside the sleeve, thus the overall strength of a grouted sleeve connection is the same as that of the rebar it connects. When the peak temperature exceeds 500 °C, the strength of a grouted sleeve connection is lower than that of a continuous rebar and the connection fails due to bond failure. Thus, the bond strength represents the strength of the connection. It is worthy of noting that bond strength decreases more quickly than the strength of continuous rebar as temperature increases. Contrary to a continuous rebar whose elastic modulus can be fully recovered when the temperature is back to normal after being exposed to fire, the reduction in elastic modulus of a grouted sleeve connection due to elevated temperature is permanent. This is because the high temperature reduces the strength of the grouting material, which may have caused internal cracking and debonding that contributes in the permanent loss of bond stiffness.

4. Comparative analysis and calculation methods

4.1 Comparisons between Path-I and Path-II

The failure modes of load Path-I are rebar rupture outside the sleeve, bond failure and rebar rupture inside the sleeve. For Path-II, all the sleeve connections fail due to rebar rupture inside and near the edge of the sleeves. The detailed analyses of the failures can be seen in Section 3.

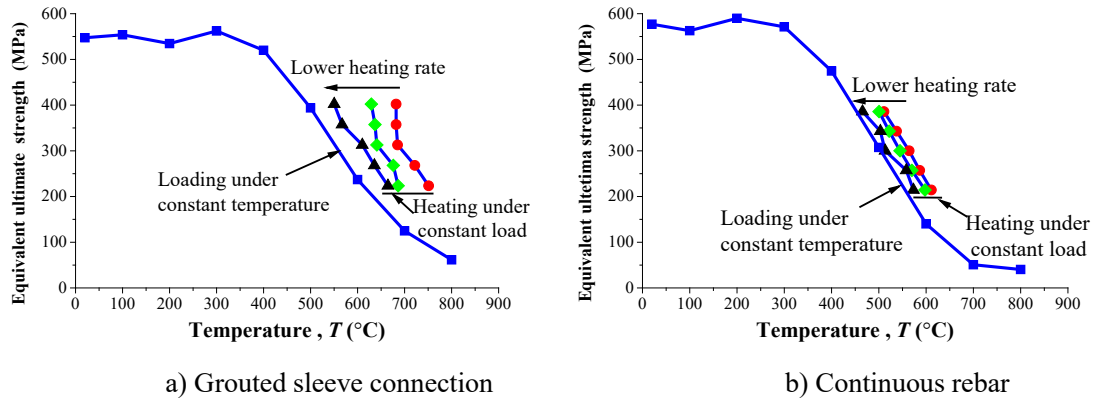


Figure 17 Comparisons of equivalent ultimate strength between Path-I and Path-II

Figures 17 (a) and (b) show comparisons of the equivalent ultimate strength at different temperature between Path-I and Path-II of the grouted sleeve connections and the continuous rebars, respectively. For the grouted sleeve connections, the low heat conduction rate of the grouting material creates a large temperature gradient between the core and the external surface of the grouted sleeves under Path-II, while there is no temperature gradient under Path-I because a uniform temperature field has been achieved after the sleeve is heated under a constant temperature for 3 hours. Therefore, high temperature performance of grouted sleeves under Path-II is higher than

under Path-I. However, this advantage is reduced as the heating rate decreases because the temperature gradient with the sleeves becomes smaller. Therefore, the fire resistance of Path-I is conservative in fire resistance design, especially when heating rate is higher. As for a continuous rebar, the high temperature performance under Path-II with a low heating rate is close to the high temperature performance under Path-I. This is due to that the cross section of the continuous rebar is very small, resulting in a smaller temperature gradient and a rather uniform distribution of temperature. Thus, the effect of heating rate on the high temperature performance under Path-II is small.

4.2 Comparisons between Path-I and Path-III

When the temperature is below 500°C, the failure modes of grouted sleeve connections under Path-I and Path-III are the same, and all the tested sleeves shows rebar rapture outside the sleeves. However, as the temperature exceeds 500°C, their failure modes are different. For grouted sleeve connections under Path-I, the failure mode changes from bond failure to rebar rapture inside the sleeves as temperature increases. For grouted sleeve connections under Path-III, the tests shown only rebar rapture inside the sleeves. The detailed of the failures have been studied in Section 3.

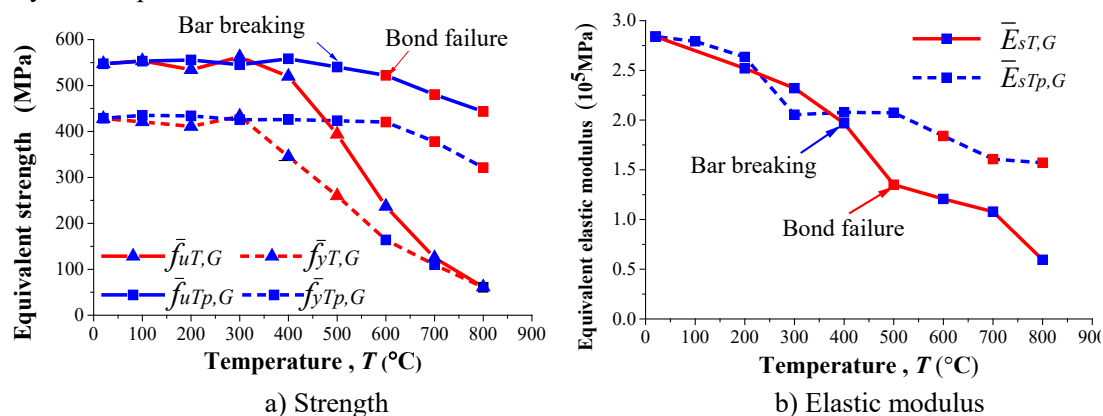


Figure 18 Comparisons of mechanical properties of grouted sleeves between Path-I and Path-III

Figure 18 (a) shows comparisons of the strength of the grouted sleeve connections at different temperature between Path-I and Path-III. For temperatures below 400°C, all the grouted sleeve connections fail due to rebar rapture outside the sleeves, thus, the strength of all the grouted sleeve connections is the same as that of the rebar at the same temperature. When the temperature reaches 500°C, the strength of the sleeves under Path-III is greater than under Path-I. The grouted sleeve connections under Path-III finally fail due to rebar rapture outside the sleeves. The grouted sleeve connections under Path-I fail due to bond failure. Therefore, the bond strength of the grouted sleeves under Path-III is higher than that under Path-I, suggesting that bond strength loss due to elevated temperature may have been partially restored. According to studies of Robins P J^[33] and Einea et al, bond strength is related to the strength of grouted material and the lateral pressure, the strength of grouted material under and after elevated temperature are close to each other^[34], however, the lateral pressure provided by sleeve under high temperature is greater than that after high temperature, thus the bond strength have partially restored. When the temperature exceeds 500°C, it can also be found that strength of the grouted sleeves under Path-III is greater than that under Path-I. Under Path-I, the tensile strength of rebar decays rapidly as the temperature increases and rebar rapture occurs eventually inside the sleeves. However, rebar rapture does not occur inside the sleeves due to the

above-mentioned restored strength of the rebar under Path-III. Figure 18 (b) shows comparison of elastic modulus of the grouted sleeve connections between Path-I and Path-III. It can be seen that the elastic modulus of the grouted sleeve connections under Path-III is greater than that under Path-I when the temperature ranges from 20 °C to 800 °C, illustrating some stiffness restoration of the grouted sleeve connections, which is related to bond strength.

4.3 Calculation methods

In this Section analytical calculation formulas are proposed on the basis of the observations from and the discussions on the experimental results.

Under Path-I, when the heating temperature is below 400 °C, the strength of the grouted sleeve connections is the same as the strength of rebar at room temperature. When the heating temperature exceeds 400 °C, the strength of the grouted sleeve connections decreases rapidly. The equivalent elastic modulus of the grouted sleeve connection decreases as the heating temperature rises from 20 °C to 800 °C. The proposed equations for equivalent strength and elastic modulus of heated grouted sleeve connection are shown in Eqs. (2)-(3) by curve fitting to the test data, as shown in Figure 19.

$$\frac{\bar{f}_{yT,G}}{\bar{f}_{y,G}} = \frac{\bar{f}_{uT,G}}{\bar{f}_{u,G}} = \begin{cases} 1 & 20^{\circ}C \leq T \leq 400^{\circ}C \\ e^{-\left(\frac{T-400}{574}\right)^{2.55}} & 400^{\circ}C \leq T \leq 800^{\circ}C \end{cases}, \quad (2)$$

$$\bar{E}_{sT,G}/\bar{E}_{s,G} = 1 - (T - 20)/1045, \quad 20^{\circ}C \leq T \leq 800^{\circ}C \quad (3)$$

Where $\bar{f}_{y,G}$ and $\bar{f}_{yT,G}$ are the equivalent yield strength of a grouted sleeve connection at room and elevated temperature T , respectively; $\bar{f}_{u,G}$ and $\bar{f}_{uT,G}$ are the respective equivalent ultimate strength of a grouted sleeve connection at room and elevated temperature T ; $\bar{E}_{s,G}$ and $\bar{E}_{sT,G}$ are the equivalent elastic modulus of a grouted sleeve connection at room and elevated temperature T . The ratios of the strength and the modulus represent their respective reduction factors that are shown by the fitted curves shown in Figures 19 and 20.

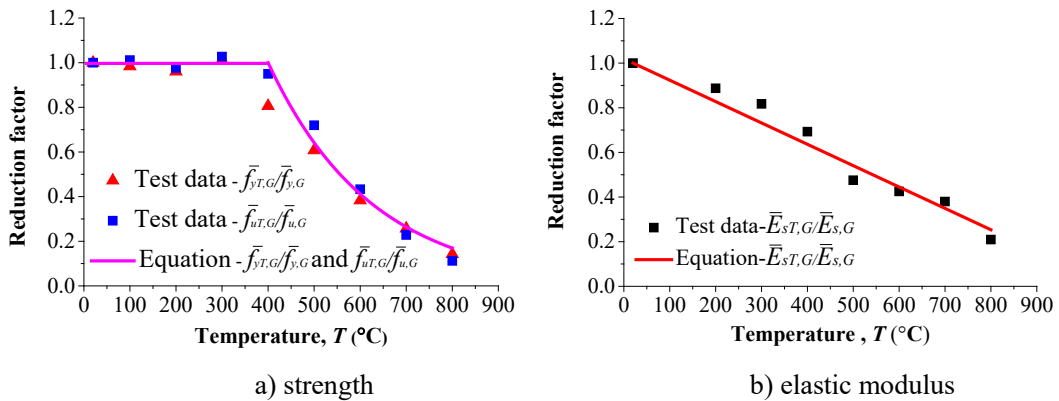


Figure 19 Curve fitting the test results of Path-I

Under Path-III, the equivalent yield strength and the equivalent ultimate strength of grouted sleeve connections do not show any difference with the strength at room temperature when the peak temperature does not exceed 500 °C and 600 °C, respectively. The equivalent yield strength and the equivalent ultimate strength of a grouted sleeve connections decreases almost linearly when the

peak temperature exceeds 500 °C and 600 °C, respectively. The equivalent elastic modulus of a grouted sleeve connections also decreases almost linearly with increase of the peak temperature. The proposed equations for equivalent strength and elastic modulus of heated connections are shown in Eqs. (4)-(7) by curve fitting to the test data, as illustrated in Figure 20.

$$\frac{\bar{f}_{yTp,G}}{\bar{f}_{y,G}} = \begin{cases} 1 & 20^{\circ}C \leq T \leq 600^{\circ}C \\ 1 - (T - 600)/1630 & 600^{\circ}C \leq T \leq 800^{\circ}C \end{cases} \quad (4)$$

$$\frac{\bar{f}_{uTp,G}}{\bar{f}_{u,G}} = \begin{cases} 1 & 20^{\circ}C \leq T \leq 500^{\circ}C \\ 1 - (T - 500)/806 & 500^{\circ}C \leq T \leq 800^{\circ}C \end{cases} \quad (5)$$

$$\bar{E}_{sTp,G} / \bar{E}_{s,G} = 1 - (T - 20)/1621 \quad , \quad 20^{\circ}C \leq T \leq 800^{\circ}C \quad (6)$$

Where $\bar{f}_{yTp,G}$, $\bar{f}_{uTp,G}$ and $\bar{E}_{sTp,G}$ are equivalent yield strength, equivalent ultimate strength and equivalent elastic modulus of a grouted sleeve connection at peak temperature T_p , respectively.

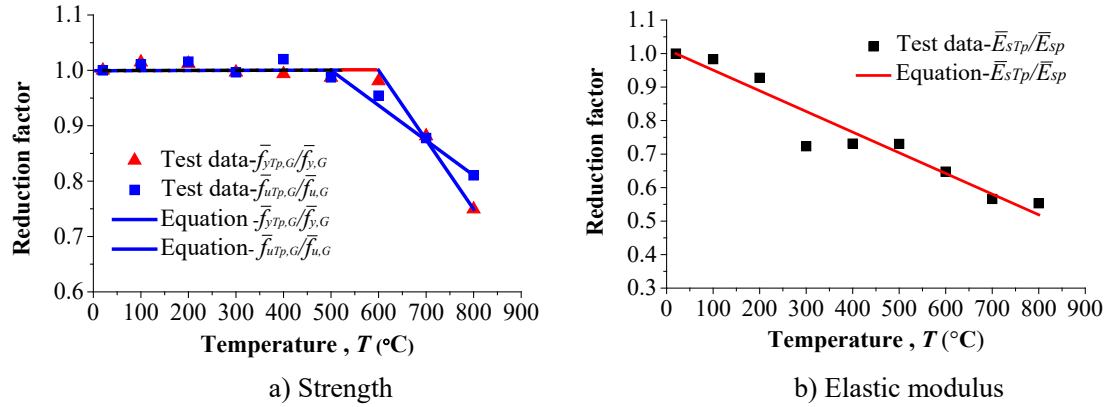


Figure 20 Curve fitting the test results of Path-III

5. Conclusions

In this paper, experimental investigations on the behavior of grouted sleeve connections under different thermal-mechanical loading paths have been presented. The load paths were proposed to meet different fire resistance design requirements. Failure modes and degradation of mechanical properties of the grouted sleeve connections were studied. On the basis of the test results, formulas for predicting strength and stiffness of the connections were proposed based on curve fitting. From the present study, the following conclusions can be drawn:

(1) Possible failure modes under Path-I loading include bond failure and rebar rapture. Rebar rapture occurred both outside and inside the sleeve. Under load Path-II, the inside rebar rapture occurs near the edge of the sleeve. The primary failure modes of a grouted sleeve connection under load Path-III are rebar rapture outside the connection and bond failure.

(2) Under load Path-I, the strength of a grouted sleeve connection is always greater than that of a continuous rebar when the heating temperature exceeds 400 °C, while the elastic modulus of a grouted sleeve connection is always greater than that of continuous rebar, independent of temperature. Under load Path-II, a grouted sleeve connection has enhanced high temperature

performance than a continuous rebar does. Under load Path-III, the strength of a grouted sleeve connection is lower than that of a continuous rebar when the peak temperature exceeds 500 °C. Contrary to a continuous rebar whose elastic modulus can be fully recovered, the reduction in elastic modulus of grouted sleeve connection is permanent.

(3) High temperature performance of a grouted sleeve under Path-II is higher than under Path-I. However, this advantage is reduced as heating rate decreases. The strength of a sleeve connection under Path- III is greater than under Path-I when temperature reaches 500°C, while the elastic modulus of the grouted sleeve connections under Path-III is always greater than that under Path-I, independent of temperature.

Acknowledgements

The authors are grateful for the financial support from the National Key Research and Development Program of China(2016YFC0701402).

References:

- [1] Yan Q, Chen T, Xie Z. Seismic experimental study on a precast concrete beam-column connection with grout sleeves. *ENG STRUCT.* 2018;155: 330-44.
- [2] Peng Y, Qian J, Wang Y. Cyclic performance of precast concrete shear walls with a mortar - sleeve connection for longitudinal steel bars. *MATER STRUCT.* 2016;49(6): 2455-69.
- [3] Tullini N, Minghini F. Grouted sleeve connections used in precast reinforced concrete construction - Experimental investigation of a column-to-column joint. *ENG STRUCT.* 2016;127: 784-803.
- [4] Belleri A, Riva P. Seismic performance and retrofit of precast concrete grouted sleeve connections. *PCI J.* 2012;57(1): 97-109.
- [5] Ling JH, Abd. Rahman AB, Ibrahim IS, Abdul Hamid Z. Behaviour of grouted pipe splice under incremental tensile load. *CONSTR BUILD MATER.* 2012;33: 90-8.
- [6] Ling JH, Abd. Rahman AB, Ibrahim IS, Abdul Hamid Z. Tensile capacity of grouted splice sleeves. *ENG STRUCT.* 2016;111: 285-96.
- [7] Yuan H, Zhenggeng Z, Naito CJ, Weijian Y. Tensile behavior of half grouted sleeve connections: Experimental study and analytical modeling. *CONSTR BUILD MATER.* 2017;152: 96-104.
- [8] Henin E, Morcous G. Non-proprietary bar splice sleeve for precast concrete construction. *ENG STRUCT.* 2015;83: 154-62.
- [9] Seo S, Nam B, Kim S. Tensile strength of the grout-filled head-splice-sleeve. *CONSTR BUILD MATER.* 2016;124: 155-66.
- [10] Liu Y, Wang Y, Fang G, Alrefaei Y, Dong B, Xing F. A preliminary study on capsule-based self-healing grouting materials for grouted splice sleeve connection. *CONSTR BUILD MATER.* 2018;170: 418-23.
- [11] China MOHA. JGJ 107-2010, Technical Specification for Mechanical Splicing of Steel Reinforcing Bars. Beijing2010.
- [12] China MOHA. JG/T 398-2012, The Grouting Coupler for Rebars Splicing. Beijing2012.
- [13] China MOHA. Cementitious grout for couple of rebar splicing. JG/T408-2013. Beijing2013.
- [14] Brnic JTGC. Mechanical testing of the behavior of steel 1.7147 at different temperatures. *STEEL*

- COMPOS STRUCT. 2014;5(17): 549-60.
- [15] Chen J, Young B. Stress – strain curves for stainless steel at elevated temperatures. ENG STRUCT. 2006;28(2): 229-39.
- [16] Da Silva LSSA. Behaviour of steel joints under fire loading. STEEL COMPOS STRUCT. 2005;6(5): 485-513.
- [17] Gardner L, Bu Y, Francis P, Baddoo NR, Cashell KA, McCann F. Elevated temperature material properties of stainless steel reinforcing bar. CONSTR BUILD MATER. 2016;114: 977-97.
- [18] HEIDARPOUR, Amin, TOFTS, Niall S, KORAYEM, Asghar H, et al. Mechanical properties of very high strength steel at elevated temperatures. FIRE SAFETY J. 2014;64(2): 27-35.
- [19] G. Q. Li JDYS. A practical approach for fire safety design of fire-resistant steel members. A practical approach for fire safety design of fire-resistant steel members. 2005;1(5): 71-86.
- [20] Topçu OB, Karakurt C. Properties of Reinforced Concrete Steel Rebars Exposed to High Temperatures. Research Letters in Materials Science. 2008;2008: 1-4.
- [21] Y. Z. Yin YCW. Analysis of behaviour of steel beams with web openings at elevated temperatures. Steel Compos. Struct. 2006;1(6): 15-31.
- [22] Malhotra HL. The effect of temperature on the compressive strength of concrete, . MAG CONCRETE RES. 1956(8): 85-94.
- [23] U S. Concrete at High Temperatures -- A General Review. FIRE SAFETY J. 1988;1(13): 55-68.
- [24] Kodur V. Properties of Concrete at Elevated Temperatures. ISRN Civil Engineering. 2014;2014: 1-15.
- [25] Diederichs U SU. Bond strength at high temperatures. MAG CONCRETE RES. 1981;115(33): 75-84.
- [26] Morley P D RR. Response of the Bond in Reinforced Concrete to High Temperatures. Magazine of Concrete Research. 1983;123(35): 67-74.
- [27] Reinforced RRMP. Further Response of the Bond in Reinforced Concrete to High Temperatures. MAG CONCRETE RES. 1985;24(35): 157-63.
- [28] Zhao XL, Ghojel J, Grundy P, Han LH. Behaviour of grouted sleeve connections at elevated temperatures. THIN WALL STRUCT. 2006;44(7): 751-8.
- [29] Wang GQ. Experimental Study on High Temperature Performance of Reinforcement Sleeve Grouting Connection, Suzhou University of Science and Technology; 2017.
- [30] Zhang W, Deng X, Zhang J, Yi W. Tensile behavior of half grouted sleeve connection at elevated temperatures. CONSTR BUILD MATER. 2018;176: 259-70.
- [31] Shi XD, Guo ZH. High temperature performance and calculation of reinforced concrete. Beijing: Tsinghua University Press, 2003.
- [32] Ingberg SH. Tests of the Severity of Building Fires. NFPA Quarterly: NFPA Quarterly, 1928.
- [33] Robins P J SIG. The effect of lateral pressure on the bond of round reinforcing bars in concrete. International Journal of Adhesion and Adhesives. 1982;2(2): 129-33.
- [34] Standardization ECF. Design of Composite Steel and Concrete Structure-Part1-21: General Rules-Structural Fire Design. 1994.